

# High Accuracy Navigation Using Laser Range Sensors in Outdoor Applications

Jose Guivant, Eduardo Nebot, Stefan Baiker

Australian Centre for Field Robotics  
Department of Mechanical and Mechatronic Engineering  
The University of Sydney, NSW 2006, Australia  
jguivant/nebot @mech.eng.usyd.edu.au

## Abstract

This paper presents the design of a high accuracy outdoor navigation system based on standard dead reckoning sensors and laser range and bearing information. The data validation problem is addressed using laser intensity information. Beacon design aspect and location of landmarks are also discussed in relation to desired accuracy and required area of operation. The results are important for Simultaneous Localization and Map building applications since the feature extraction and validation are resolved at the sensor level using laser intensity. This facilitates the use of additional natural landmarks to improve the accuracy of the localization algorithm. Experimental results in outdoor environments are also presented.

## 1 Introduction

Reliable localization is an essential component of any autonomous vehicle. The basic navigation loop is based on dead reckoning sensors that predict the vehicle high frequency manoeuvres and low frequency absolute sensors that bound the positioning errors [1]. Although there are a wide variety of external sensors, only few of them can be used in a particular application and the reliability will be function of the environment of operation, [2].

It is well known that with the different type of GPS implementations we can obtain position fixes with errors of the order of 2cm to 100m, [3]. Nevertheless this accuracy cannot be guarantee all the time in most working environment where partial satellite occlusion and multipath effects can prevent normal GPS receiver operation. Similar problems are experienced with some other type of sensors such as Stereo Vision, Ultrasonic, Laser and Radars. A significant amount of work has been devoted to the use of range and bearing sensors for localization purposes. Ultrasonic sensors have been widely used in indoor applications [4], but they are not adequate for most outdoor applications due to range limitations and bearing uncertainties. Stereovision has been the object of research in many important research laboratories around the world. But its complexity and its poor dynamic range made this technique still not very reliable for outdoor applications. Millimeter Wave Radar [5], is an emerging technology that has enormous potential for obstacle detection, map building and navigation in indoor and outdoor applica-

tions. The main drawback of this technology is its actual cost but this is expected to change in the near future. Range and bearing lasers have become one of the most common sensors for localization and map building purposes due to their accuracy and low cost. Most common lasers provide range and bearing information with sub degree resolution and accuracies of the order of 1-10 cm in 10-50 meter ranges.

One of the most difficult problems for any beacon localization algorithm is not feature extraction, but feature validation and data association. That is to confirm that the extracted feature is a valid feature and to associate it with a known or estimated feature in the world map. Data association is essential for the SLAM problem. This problem has been addressed in previous works using redundancy information by looking for stable features [6], or using a combination of sensors such as in [7], where vision information is used to validate certain type of features extracted from laser information.

This work makes use of laser intensity information to recognize landmarks. It demonstrates that high accurate localization can be obtained with this information. These results are essential to incorporate additional natural landmarks and to facilitate SLAM application. The navigation algorithm is implemented in information form. This algorithm becomes more attractive that the standard Kalman filter for application where the external information is available from different sources and at different times [1].

## 2 Navigation loop

The navigation loop is based on encoders and range/ bearing information provided by a Sick laser sensor. The models for the process and observation are non-linear. The encoders provide velocity and steering angle information that is used with a kinematic model of the vehicle to predict position and orientation. The prediction is updated with external range and bearing information provided by a laser system.

### Modelling Aspect

A simple kinematic model is used for this experimentation. This model can be extended to consider other pa-

rameters such as wheel radius and slip angle that can have significant importance in other applications [8].

The vehicle position is represented in global coordinates as shown in Figure 1. The steering control  $\alpha$  is defined in vehicle coordinate frame. The laser sensor is located in the front of the vehicle and returns range and bearing related to objects at distances of up to 50 meters. High intensity reflection can be obtained by placing high reflectivity beacons in the area of operation. These landmarks are labeled as  $Bi_{(i=1..n)}$  and measured with respect to the vehicle coordinates  $(x_L, y_L)$ , that is  $z(k) = (r, \beta, I)$ , where  $r$  is the distance from the beacon to the laser,  $\beta$  is the sensor bearing measured with respect to the vehicle coordinate frame and  $I$  is the intensity information.

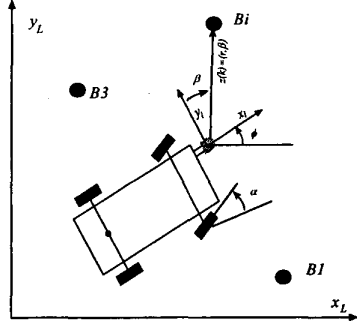


Figure 1 Vehicle coordinate system

Considering that the vehicle is controlled through a demanded velocity  $v_c$  and steering angle  $\alpha$  then the process model that predict the trajectory of the centre of the back axle is given by

$$\begin{bmatrix} \dot{x}_c \\ \dot{y}_c \\ \dot{\phi}_c \end{bmatrix} = \begin{bmatrix} v_c \cdot \cos(\phi) \\ v_c \cdot \sin(\phi) \\ \frac{v_c}{L} \cdot \tan(\alpha) \end{bmatrix} \quad (1)$$

The laser is located in the front of the vehicle. To facilitate the update stage the kinematic model of the vehicle is designed to represent the trajectory of the centre of the laser. Based on Figure 1 and 2, the translation of the centre of the back axle can be given

$$P_L = P_C + a \cdot \vec{T}_\phi + b \cdot \vec{T}_{\phi + \pi/2} \quad (2)$$

Being  $P_L$  and  $P_C$  the position of the laser and the centre of the back axle respectively. The transformation is defined by the orientation angle, according to the following vectorial expression:

$$\vec{T}_\phi = (\cos(\phi), \sin(\phi)) \quad (3)$$

The scalar representation is

$$\begin{aligned} x_L &= x_c + a \cdot \cos(\phi) + b \cdot \cos\left(\phi + \frac{\pi}{2}\right) \\ y_L &= y_c + a \cdot \sin(\phi) + b \cdot \sin\left(\phi + \frac{\pi}{2}\right) \end{aligned} \quad (4)$$

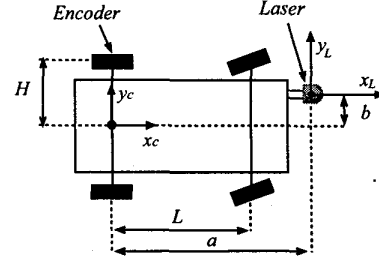


Figure 2 Kinematics parameters

Finally the full state representation can be written

$$\begin{bmatrix} \dot{x}_L \\ \dot{y}_L \\ \dot{\phi}_L \end{bmatrix} = \begin{bmatrix} v_c \cdot \cos(\phi) - \frac{v_c}{L} \cdot (a \cdot \sin(\phi) + b \cdot \cos(\phi)) \cdot \tan(\alpha) \\ v_c \cdot \sin(\phi) + \frac{v_c}{L} \cdot (a \cdot \cos(\phi) - b \cdot \sin(\phi)) \cdot \tan(\alpha) \\ \frac{v_c}{L} \cdot \tan(\alpha) \end{bmatrix} \quad (5)$$

The velocity is generated with an encoder located in the back left wheel. This velocity is translated to the centre of the axle with the following equation:

$$v_c = \frac{v_e}{\left(1 - \tan(\alpha) \cdot \frac{H}{L}\right)} \quad (6)$$

Where for this car  $H = 0.75\text{m}$ ,  $L = 2.83\text{m}$ ,  $b = 0.5$  and  $a = L + 0.95\text{m}$ . Finally the discrete model in global coordinates becomes

$$\begin{bmatrix} x(k) \\ y(k) \\ \phi(k) \end{bmatrix} = \begin{bmatrix} x(k-1) + \Delta t v_c(k-1) \cdot \cos(\phi(k-1)) - \\ \frac{v_c(k-1)}{L} \cdot (a \cdot \sin(\phi(k-1)) + b \cdot \cos(\phi(k-1))) \\ \cdot \tan(\alpha(k-1)) \\ y(k-1) + \Delta t v_c(k-1) \cdot \sin(\phi(k-1)) + \\ \frac{v_c(k-1)}{L} \cdot (a \cdot \cos(\phi(k-1)) - b \cdot \sin(\phi(k-1))) \\ \cdot \tan(\alpha(k-1)) \\ \frac{v_c(k-1)}{L} \cdot \tan(\alpha(k-1)) \end{bmatrix} \quad (7)$$

where  $\Delta T$  is the sampling time, that in our case is not constant. The process can then be written as a nonlinear equation

$$\begin{aligned} X(k) &= f(X(k-1), u(k-1)) + \mu(k-1) + \omega_f(k-1) \\ X(k) &\approx f(X(k-1), u(k-1)) + \omega_u(k-1) + \omega_f(k-1) \end{aligned} \quad (8)$$

where  $X(k-1)$  and  $u(k-1)$  are the estimate and input at time  $k-1$  and  $\mu(k-1)$ ,  $\omega_f(k-1)$  are process noises. The process noise is mainly due to measurement errors in the velocity and steering input information. The model for  $\omega_u(k)$  is given by:

$$[\omega_u(k)] = [\nabla f_{u(k-1)}(X, u)] \cdot \mu(k) \quad (9)$$

where  $\nabla f_u = \frac{\partial f}{\partial u} = \frac{\partial(x, y, \phi)}{\partial(u_1, u_2)}$  is the gradient of  $f$  with re-

spect to the input  $u = (u_1, u_2) = (v, \alpha)$  and  $\mu(k)$  is gaussian noise. The equation that relates the observation with the states is

$$\begin{bmatrix} z_r^i \\ z_\beta^i \end{bmatrix} = h(X, x_i, y_i) = \begin{bmatrix} \sqrt{(x_L - x_i)^2 + (y_L - y_i)^2} \\ \text{atan}\left(\frac{(y_L - y_i)}{(x_L - x_i)}\right) - \phi + \pi/2 \end{bmatrix} \quad (10)$$

where  $z$  and  $[x, y, \phi]$  are the observation and state values respectively, and  $(x_i, y_i)$  are the known positions of the beacons or natural landmarks. The observation equation can be expressed in short form as

$$z(k) = h(x(k)) + \eta(k) \quad (11)$$

with

$$\eta(k) = \begin{bmatrix} \eta_R(k) \\ \eta_\beta(k) \end{bmatrix} \quad (12)$$

The noises  $\mu(k)$  and  $\eta(k)$  are assumed to be Gaussian, temporally uncorrelated and zero mean, that is

$$E[\mu(k)] = E[\eta(k)] = 0 \quad (13)$$

with corresponding covariance

$$E[\mu(i)\mu^T(j)] = \delta_{ij} Q_{\alpha v}(i), E[\eta(i)\eta^T(j)] = \delta_{ij} R_{r, \beta}(i) \quad (14)$$

### 3 Simultaneous Localization and Map Building

The localization and map building problem can also be approached with this combination of sensors. In this case the estimated location of the features or beacons becomes part of the state vector. The vehicle starts at an unknown position with a given uncertainty and obtains measurements of the environment relative to its position. This information is used to incrementally build and maintain a navigation map and localize with respect to this map.

The state vector is now given by:

$$X = \begin{bmatrix} x_v \\ x_L \end{bmatrix} \quad (15)$$

$$x_v = (x, y, \phi) \in R^3$$

$$x_L = (x_1, y_1, \dots, x_n, y_n) \in R^N$$

where  $x_v$  and  $x_L$  are the states of the vehicle and actual landmarks. The landmarks can be natural features and special designed beacons located at unknown location. The dynamic model of the extended system that considers the new states can now be written:

$$\begin{aligned} x_v(k+1) &= f(x_v(k)) \\ x_L(k+1) &= x_L(k) \end{aligned} \quad (16)$$

It can be seen that the dynamic of the states  $x_L$  is invariant since the landmarks are assumed to be static. Then the Jacobian matrix for the extended system becomes

$$\frac{\partial F}{\partial X} = \begin{bmatrix} \frac{\partial f}{\partial x_v} & \emptyset \\ \emptyset^T & I \end{bmatrix} = \begin{bmatrix} J_1 & \emptyset \\ \emptyset^T & I \end{bmatrix} \quad (17)$$

$$J_1 \in R^{3 \times 3}, \quad \emptyset \in R^{3 \times N}, \quad I \in R^{N \times N}$$

The observation obtained with a range and bearing device are relative to the vehicle position. The observation equation includes the state of the vehicle and the states representing the position of the landmark:

$$\begin{aligned} r_i = h_r(X) &= \|(x, y) - (x_i, y_i)\|_2 = \sqrt{(x - x_i)^2 + (y - y_i)^2} \\ \alpha_i = h_\alpha(X) &= \text{atan}\left(\frac{(y - y_i)}{(x - x_i)}\right) - \phi + \frac{\pi}{2} \end{aligned} \quad (18)$$

where  $(x, y)$  is the position of the vehicle,  $(x_i, y_i)$  the position of the landmark numbered  $i$  and  $\phi$  the orientation of the car.

Then the Jacobian matrix of the vector  $(r_i, \alpha_i)$  respect to the variables  $(x, y, \phi, x_i, y_i)$  can be evaluated using:

$$\frac{\partial h}{\partial X} = \begin{bmatrix} \frac{\partial h_r}{\partial X} \\ \frac{\partial h_\alpha}{\partial X} \end{bmatrix} = \begin{bmatrix} \frac{\partial r_i}{\partial(x, y, \phi, \{x_i, y_i\})} \\ \frac{\partial \alpha_i}{\partial(x, y, \phi, \{x_i, y_i\})} \end{bmatrix} \quad (19)$$

with

$$\begin{aligned} \frac{\partial h_r}{\partial X} &= \frac{1}{\Delta} \cdot [\Delta x, \Delta y, 0, 0, 0, \dots, -\Delta x, -\Delta y, 0, \dots, 0, 0] \\ \frac{\partial h_\alpha}{\partial X} &= \left[ -\frac{\Delta y}{\Delta^2}, \frac{\Delta x}{\Delta^2}, -1, 0, 0, \dots, \frac{\Delta y}{\Delta^2}, -\frac{\Delta x}{\Delta^2}, 0, \dots, 0, 0 \right] \end{aligned} \quad (20)$$

$$\Delta x = (x - x_i), \quad \Delta y = (y - y_i), \quad \Delta = \sqrt{(\Delta x)^2 + (\Delta y)^2}$$

These equations can be used to build and maintain a navigation map of the environment and to track the position of the vehicle. Previous results have shown that the initial uncertainty of the vehicle cannot be reduced but can be bounded as shown later in this paper.

#### 4 Range/Bearing/Intensity laser information

This section presents the description of the laser and the beacon design aspects. The laser used in this experiment is the LMS200 model manufactured by SICK. It can return up to 361 range values spaced 0.5 degrees. The current version returns intensity information with eight different levels. This information is used to detect beacons. The laser returns intensity information only from surface with high reflectivity. This information is extremely reliable and becomes of fundamental importance for navigation purposes.

The beacon design is of fundamental importance for the successful operation of the system. Type of material, size and shape of the reflector will determine the range and accuracy of the navigation system. For this purpose it is essential to characterize the laser beam. A set of experiments was designed to obtain the laser parameters. A retroreflective tape (1.5x15cm) was radially moved at a constant distance  $R$  in steps of 5mm perpendicular to the laser beam. The Intensity output of the scanner was recorder for different radius. The results corresponding to two different radius are shown in figures 3 and 4.

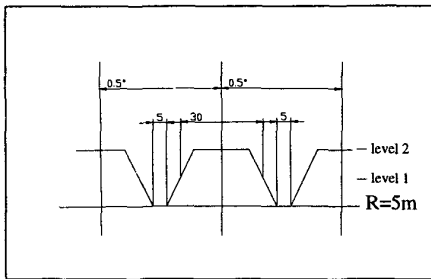


Figure 3. Intensity at 5m, beam  $\varnothing \approx 30$ mm, shadow 5 mm ( 5mm reflector)

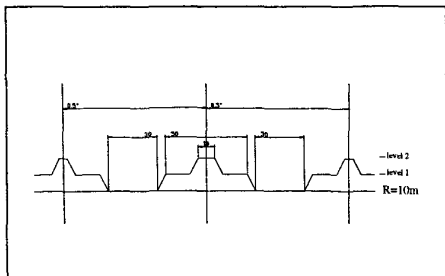


Figure 4. Intensity at 10m, beam  $\varnothing \approx 50$ mm, shadow 30 mm. ( 5mm reflector)

With this information the angular resolution of the scanner as well as the opening angle of the beam was evaluated. The characterization of the laser obtained is shown in Figure 5. The beam angle becomes approximately 0.2 degrees. This determines the minimum area of a beacon

that will be able to return maximum intensity at a given distance.

In our experimentation we used standard diamond grade reflective tape. It was determined that the laser was able to detect beacons at distances of over 35 meters with reflectors with an area of 900 cm<sup>2</sup>.

The size and shape of the beacon also becomes important when high accuracy is required. The main problem is that the landmarks will be detected several times at shorter distances.

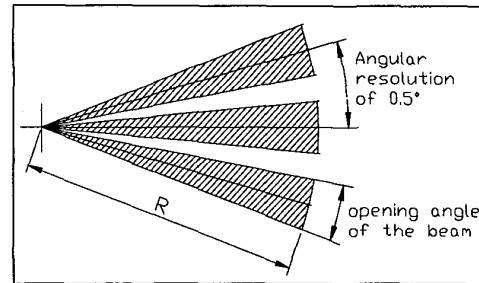


Figure 5 Laser Characteristics

This problem is shown in Figure 6 for a flat and cylindrical reflector. It can be seen that depending of the orientation and position of the vehicle the same beacon will be detected a different locations. The beacon shape is also of importance to be able to see the landmarks from different vehicle orientations. The cylinder shape shown in Figure 6 becomes very attractive for visibility purposes but it can generate different range and bearing returns depending on the position of the vehicle. These problems make the detection of landmarks less accurately at longer ranges. For each application the final selection of the shape of the landmark will depend on the number of landmarks, the required accuracy and the area of operations in relation to the characteristic of the laser.

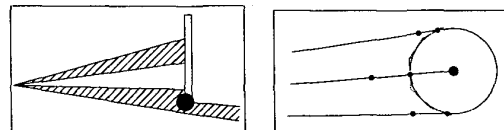


Figure 6 Bearing and range uncertainties

This section presented the main characteristics of the laser scanner and addressed the beacon design problem. This information is essential to evaluate the maximum accuracy that can be obtained with this navigation system.

#### 5 Results

The navigation system was tested with a utility vehicle retrofitted with the sensors described. A map of the testing site (landmarks positions) and a typical car trajectory is shown in Figure 7 while the vehicle was driven at speed

of up to 4 m/sec. The runs were done in the top level of the car park building of the university campus. A kinematic GPS of 2 cm accuracy was used to generate ground truth information. The "stars" in the map represent potential natural landmarks and the "circles" are the beacons. Although this environment is very rich with respect to the number of natural landmarks, the data association becomes very difficult since most of the landmarks are very close together. Under a small position error the navigation algorithm will not be able to associate the extracted features correctly. The inclusion of beacons becomes equivalent to the introduction of a different type of landmark that is validated at the sensor level. This will make the data association of the natural landmark possible with the potential of a significant reduction of the localization error. Figure 8 presents the 95 % confidence bounds of the estimated position of the vehicle, continuous line, with the true error, dotted line of the localization algorithm using beacons at known positions. It can be seen that most of the errors are bounded by the 95 % confidence bounds estimated by the filter. It is also important to note that the localizer is able to estimate the position of the vehicle with an error of approximate 6 centimetres. This is a very important achievement considering the systematic errors present in the surveying and detection of the landmarks and vehicle model errors. The second experimental results correspond to SLAM using only beacons. In this case it is not necessary to survey the position of the beacons. This information is obtained while the vehicle navigates. The system builds a map of the environment and localizes itself. The accuracy of this map is determined by the initial uncertainty of the vehicle and the quality of the combination of dead reckoning and external sensors. In this experimental results an initial uncertainty of 10 cm in coordinates  $x$  and  $y$  was assumed. Figure 9 presents the absolute error and the predicted standard deviation ( $2\sigma$  bounds, 95 % confidence bounds). This plot shows that the bounds are consistent with the actual error. It is also important to remark that the uncertainty in position does not reduce below the initial uncertainty. This is expected since the laser information is obtained relative to the vehicle position. The landmark covariance estimation is shown in Figure 10. This figure presents the variance of position  $x$  and  $y$  and the estimated uncertainty of a selected group of landmarks. The ones with oscillatory behaviour correspond to the uncertainty of the vehicle. The original uncertainty of a new landmark will be a function of the actual vehicle uncertainty and sensor noise. It can also be appreciated from this plot that due to the correlation of the map all landmarks are being updated all the time. The final experimental results correspond to SLAM using all the features available in the environment. In this case it is not required to modify the infrastructure of the environment with the addition of beacons. The most relevant navigation features are obtained while the vehicle navigates. Figure 11 shows the initial part of the experimental run while the system is still incorporating new landmarks. Figure 12 presents the absolute error with the

predicted standard deviation ( $2\sigma$  bounds, 95 % confidence bounds). This figure shows that the bounds obtained using all landmarks are consistent with the actual errors. It is also important to remark that the uncertainty in position become significantly smaller than the SLAM with beacons only. This is due to a larger number of landmarks that incorporate more information to the filter.

## 6 Conclusion

This work presented the implementation of different types of high accuracy navigation algorithms for outdoor and indoor applications. A full implementation of SLAM using beacons and natural features is also presented. This is an important contribution since it does not require any surveying of the beacons. The actual results have shown that the SLAM algorithms can deliver an accuracy comparable with the standard localization algorithms. It was also demonstrated that the algorithm successfully build and maintain a map for long runs. This experimental results presented a 3 km run and the algorithm remains stable. We are currently investigating more efficient implementations of this algorithm taking into consideration the sparseness of the matrix involved in SLAM.

## References

- [1] Nebot E., Durrant-Whyte H., "High Integrity Navigation Architecture for Outdoor Autonomous Vehicles", *Journal of Robotics and Autonomous Systems*, Vol. 26, February 1999, p 81-97.
- [2] Nebot E., "Sensors used for autonomous navigation", *Advances in Intelligent Autonomous Systems*, Chapter 7, pp. 135-156, ISBN 0-7923-5580-6, March 1999, Kluwer Academic Publishers, Dordrecht.
- [3] Sukkarieh S., Nebot E., Durrant-Whyte H., "A High Integrity IMU/GPS Navigation Loop for Autonomous Land Vehicle applications", *IEEE Transaction on Robotics and Automation*, June 1998, p 572-578.
- [4] Elfes A., "Sonar based real-world mapping navigation", *IEEE J. Rob. Autom.*, 3(3), p 249-265, 1987.
- [5] Clark S., H. Durrant-Whyte, "Autonomous land vehicle navigation using millimeter wave radar", *Int. Proc. of the IEEE Intern. conference of Robotic and Automation*, Belgium, May 1998, p 3697-3792.
- [6] Clark S., Dissanayake G., "Simultaneous Localisation and Map Building Using Millimetre Wave Radar to Extract Natural Features", 1998 IEEE Conf. on Rob. and Autom., Detroit, USA 1999, pp 1316-1321.
- [7] Perez J., Castellanos J., Montiel J., Neira J., Tardos J., "Continuous Mobile Robot Localization: Vision vs. Laser", *Proc. Of the 1999 IEEE Conference on Robotics and Automation*, p 2917-2923.
- [8] Scheding S., Dissanayake, Nebot E., Durrant-Whyte H., "An Experiment in Autonomous Navigation of an Underground Mining Vehicle", *IEEE Transaction on Rob. and Automation*, Vol. 15, No 1, Feb. 1999, p 85-95.

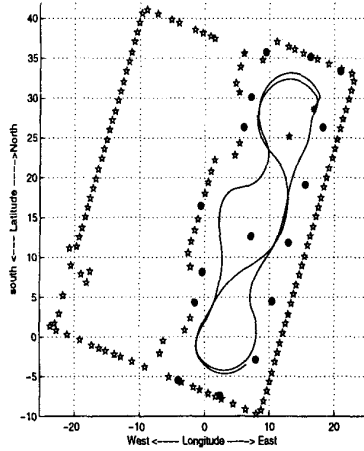


Figure 7 Landmark Positions and a typical trajectory

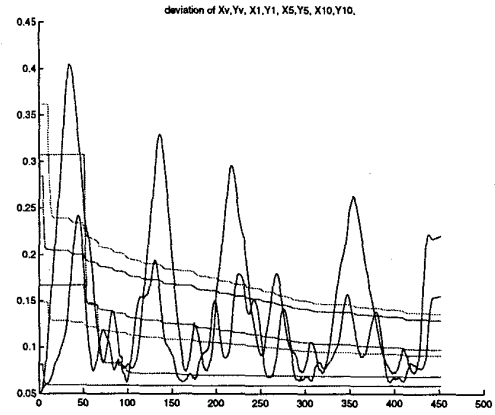


Figure 10 Estimated deviation of position and beacons

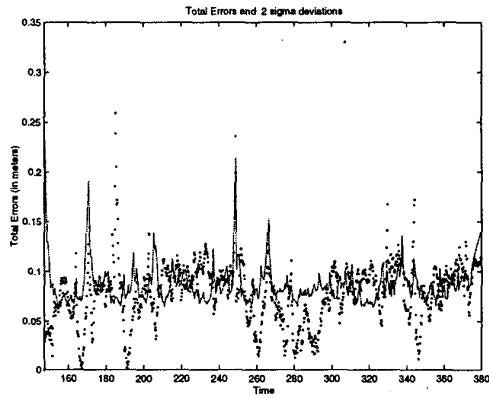


Figure 8 Standard deviation with beacons

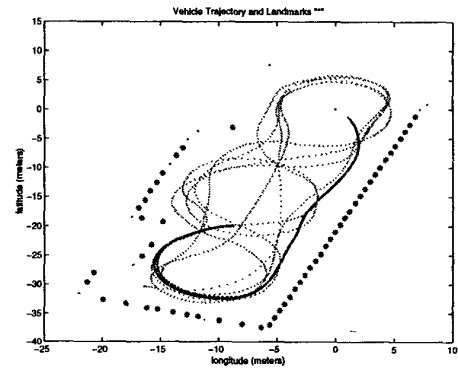


Figure 11. Initial part of the trajectory using SLAM with beacons

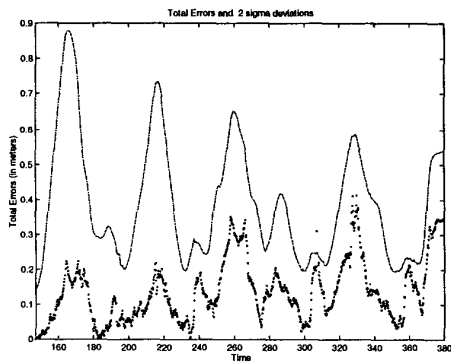


Figure 9 Absolute position error and standard deviation.

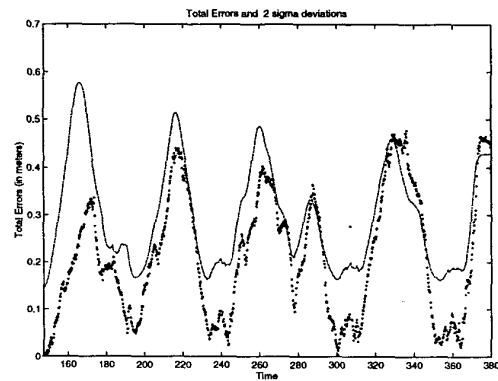


Figure 12 Absolute position error and standard deviation.